Impact of poleward heat and moisture transports on Arctic clouds and climate simulation

Eun-Hyuk Baek[1], Joo-Hong Kim[2], Sungsu Park[3*], Baek-Min Kim[4*], Jee-Hoon Jeong[1]

[1]Faculty of Earth and Environmental Sciences, Chonman National University, 77 Yongbong-ro, Buk-gu Gwangju, 61186, South Korea

[2]Unit of Arctic Sea-Ice Prediction, Korea Polar Research Institute, 26 Songdomirae-ro, Yeonsu-gu, Incheon, 21990, South Korea

[3]School of Earth and Environmental Sciences, Seoul National University, 1 Gwanak-ro, Gwanak-gu, Seoul, 08826, South Korea

[4]Department of Environmental Atmospheric Sciences, Pukyong National University, 49 Yongso-ro, Nam-gu, Busan, 48513, South Korea

Correspondence to: Sungsu Park (sungsup@snu.ac.kr) and Baek-Min Kim (baekmin@pknu.ac.kr)

Abstract. Clouds play an important role in regulating the Earth's global radiation budget. Many General Circulation Models (GCMs) have difficulty in simulating Arctic clouds and climate with a large inter-model spread. In an attempt to address this issue, we compare an Atmospheric Model Inter-comparison Project (AMIP) simulation from the Community Atmosphere Model version 5 (CAM5) with that from the Seoul National University (SNU) Atmosphere Model version 0 with a Unified Convection Scheme (SAM0). Over the Arctic, it was found that SAM0 simulates more cloud fraction and cloud liquid mass than CAM5, reducing the Arctic clouds biases in CAM5. The budget analysis indicates that this improvement is associated with an enhanced net condensation rate of water vapor into the liquid condensate of the Arctic low-level stratus, which in turn is driven by enhanced poleward transports of heat and moisture by mean meridional circulation and transient eddies. The reduced Arctic cloud biases lead to improved simulations of surface radiation fluxes and near-surface air temperature over the Arctic throughout the year. The association between the enhanced poleward transports of heat and moisture and more liquid stratus over the Arctic is also evident in the multi-models analysis. Our study indicates that the proper simulation of poleward heat and moisture transport is one of the key factors necessary for improving the simulations of Arctic clouds and climate.

1. Introduction

With increasing greenhouse gases, the Arctic has undergone the most rapid warming on Earth. During the last decade, the warming rate of near-surface air temperature over the Arctic has been two to three times of that of the entire globe (Johannessen et al., 2016; Screen and Simmonds, 2010; Serreze and Barry, 2011). This pronounced Arctic temperature amplification, some of which is forced by the positive feedbacks among various climate components (e.g., sea ice albedo feedback (Deser et al., 2000), water vapor and cloud feedback (Lu and Cai, 2009), lapse-rate feedback (Pithan et al., 2014)), is also responsible for extreme weather and climate events over mid-latitude continents (Kug et al., 2015; Screen and Simmonds, 2013; Wu and Smith, 2016). Most General Circulation Models (GCMs) have trouble in properly simulating the Arctic climate, suffering from the excessive cold surface temperature. The inter-GCM spread of greenhouse-induced warming is the largest over the Arctic (Boe et al., 2009; de Boer et al., 2012; Chapman and Walsh, 2007; Karlsson and Svensson, 2013). Many studies

reported that the GCM-simulated cold biases over the Arctic are associated with the biases of shortwave (SW) and longwave (LW) radiations at the surface, which are mainly due to poor simulation of Arctic clouds (Barton et al., 2014; English et al., 2015; Karlsson and Svensson, 2013; Shupe and Intrieri, 2004).

Over the Arctic, many GCMs underestimate the cloud fraction (de Boer et al., 2012; Cesana and Chepfer, 2012; English et al., 2015; Kay et al., 2016) and cloud liquid mass (Cesana et al., 2015; English et al., 2014; Kay et al., 2016). Because the liquid-containing clouds (i.e., mixed-phase clouds) have a larger optical depth than the pure ice clouds (King et al., 2004; Shupe and Intrieri, 2004), less cloud liquid mass causes weaker cloud radiative forcing in GCMs. Unlike in the midlatitudes, the mixed-phase clouds over the Arctic can persist for several days (Morrison et al., 2011; Shupe et al., 2011). From a process point of view, cloud liquid in the mixed-phase clouds should be rapidly depleted into cloud ice within a few hours owing to the higher saturation vapor pressure over water than over ice (i.e., the Wegener–Bergeron–Findeisen (WBF) mechanism) (Bergeron, 1935; Findeisen, 1938; Wegener, 1911). Therefore in order to sustain cloud liquids for several days, a certain production mechanism needs to counteract the WBF depletion process. Morrison et al. (2011) reviewed various candidate production processes for cloud liquid in the Arctic mixed-phase clouds, such as the compensating feedback between the formation and growth of cloud liquid droplets and ice crystals (Jiang et al., 2000; Prenni et al., 2007), in-cloud turbulence generated by cloud top radiative cooling (Korolev and Field, 2008; Shupe et al., 2008), and horizontal advection by large-scale flows (Sedlar and Tjernström, 2009; Solomon et al., 2011). More recent studies also noted that ice nucleation may be important for correctly simulating Arctic mixed-phase clouds. Liu et al. (2011) showed that their revised ice nucleation scheme increases cloud liquid mass in the Arctic mixed-phase stratocumulus and associated downward LW flux at the surface during the Fall 2004 Mixed-Phase Arctic Cloud Experiment (MPACE). Subsequent sensitivity studies with various ice nucleation schemes reported similar results (English et al., 2014; Xie et al., 2013). These improvements are attributed to the slow-down of the WBF depletion process in mixed-phase clouds with the revised ice nucleation. Even though cloud liquid mass increased, however, low-level cloud fraction decreased in their simulations, such that the biases of the radiation fluxes at the surface and the top-of-atmosphere (TOA) still remained.

As an attempt to sort out the factors responsible for the negative biases in GCM-simulated cloud liquid mass and cloud fraction over the Arctic, in this study, we compare the Arctic climate simulated by the Seoul National University Atmosphere Model version 0 with a Unified Convection Scheme (SAM0-UNICON; Park, 2014a, 2014b; Park et al., 2017; Park et al., 2019) with that of the Community Atmosphere Model version 5 (CAM5; Neale et al., 2012; Park et al., 2014). By comparing two Atmospheric Model Intercomparison Project (AMIP) simulations with CAM5 and SAM0-UNICON, we will show that SAM0-UNICON simulates cloud fraction, cloud liquid mass, and associated climates over the Arctic better than CAM5, mainly due to enhanced poleward transports of moisture and heat from the sub-Arctic region by mean meridional circulation and transient eddies. It will be also shown that a similar proportional relationship exists between the poleward transports of heat and moisture and Arctic cloudiness in other CMIP5 models, supporting our conclusion.

2. Method

2.1 Model and experimental design

The SAM0-UNICON (Park et al., 2019; hereinafter, SAM0, for simplicity) is one of the international GCMs participating in the Coupled Model Intercomparison Project 6 (CMIP6) (Eyring et al., 2016). SAM0 is based on CAM5 but adopts the Unified Convection Scheme (UNICON) (Park, 2014a, 2014b) instead of the CAM5's shallow (Park and Bretherton, 2009) and deep convection schemes (Zhang and McFarlane, 1995), and has a revised treatment of the cloud macrophysics process (Park et al., 2017). UNICON is a process-based subgrid convection parameterization scheme consisting of multiple convective updrafts, convective downdrafts, and subgrid cold pools and mesoscale organized flow without relying on any equilibrium constraints, such as convective available potential energy (CAPE) or convective inhibition (CIN) closures. UNICON simulates all dry-moist, forced-free, and shallow-deep convection within a single framework in a seamless, consistent, and unified way (Park, 2014a, 2014b). The revised cloud macrophysics scheme diagnoses additional detrained cumulus by assuming a steady state balance between the detrainment rate of cumulus condensates and the dissipation rate of detrained condensates by entrainment mixing (Park et al., 2017). It was shown that the addition of detrained cumulus substantially improves the simulation of low-level clouds and the associated cloud radiative forcing in the subtropical trade cumulus regime. Park et al. (2019) showed that the global mean climate, 20th century global warming, and El Nino and Southern Oscillation (ENSO) simulated by SAM0 are roughly similar to those of CAM5 and the Community Earth System Model version 1 (CESM1; Hurrell et al., 2013); however, SAM0 substantially improves the simulations of the Madden-Julian Oscillation (MJO) (Madden and Julian, 1971), diurnal cycle of precipitation, and tropical cyclones, all of which are known to be extremely difficult to simulate in GCMs.

In order to evaluate the impact of SAM0 on the Arctic cloud system, we conducted five ensemble experiments of an AMIP simulation for 36 years from January 1979 to February 2015 at a horizontal resolution of 1.9° latitude x 2.5° longitude for both CAM5 and SAM0, and compared the climatology from the two simulations over the Arctic. The detailed settings of the AMIP simulations are identical to those described in Park et al. (2014). For a fair comparison with satellite observation data, the model cloud fraction was calculated using the Cloud Feedbacks Model Intercomparison Project (CFMIP) Observation Simulator Package (COSP) diagnostic model. A detailed description of the COSP diagnostic model can be found in Kay et al. (2012).

2.2 Observational data

The observed Arctic cloud fraction and condensate phase information are from the Cloud-Aerosol Lidar and Infrared Pathfinder Satellite Observations (CALIPSO)-GCM-Oriented CALIPSO Cloud Product (CALIPSO-GOCCP) from June 2006 to November 2010 (Chepfer et al., 2010). CALIPSO-GOCCP is a high-quality satellite observation of polar clouds because it can detect optically-thin clouds without relying on the albedo or thermal contrast (Cesana and Chepfer, 2012; Kay et al., 2012). The observed TOA fluxes are from the latest version of the Clouds and Earth's Radiant Energy System (Wielicki et al., 1996) Energy Balanced and Filled data (Loeb et al., 2009) (CERES-EBAF) from March 2000 to February 2013. The observed Arctic near-surface air temperature at a 2 m height (T_{2m}) is from the European Center for Medium-Range Weather Forecasts (ECMWF) ERA-Interim reanalysis dataset from January 1979 to February 2015 (Dee et al., 2011).

2.3 CMIP5 models

In order to identify the relationship between the Arctic clouds and poleward transports of moisture and heat, we also analyzed AMIP simulations of the Coupled Model Intercomparison Project Phase 5 (CMIP5) (Taylor et al., 2012). We used the outputs from nine models (e.g., bcc-csm1-1-m, CanAM4, CNRM-CM5, GFDL-CM3,

5   HadGEM2-A, IPSL-CM5A-MR, IPSL-CM5B-LR, MIROC5, MPI-ESM-LR) which can be accessed from http://pcmdi.llnl.gov/. We selected these models based on the availability of the following model outputs: monthly low-cloud fraction calculated by CALIPSO COSP diagnostic model (variable name: cllcalipso), liquid water path (variable name: clwvi), ice water path (variable name: clivi), daily meridional wind (variable name: va), air temperature (variable name: ta), and specific humidity (variable name: hus).

10   ## 3. Results

3.1 Arctic clouds and their relationships with poleward moisture and heat transports

Figure 1a shows the annual cycle of the total cloud fraction (TCA) averaged over the Arctic area (north of 65° N) obtained from CAM5, SAM0, and the observation. Consistent with Kay et al. (2012) and English et al. (2014), CAM5 underestimates the observed TCA throughout the year. The negative biases in the CAM5-simulated TCA

15   are reduced in SAM0, which simulates a more realistic TCA, particularly during the summer. SAM0 improves not only the cloud fraction but also the simulation of cloud phase characteristics. Cesana et al. (2015) proposed the height at which the ratio of cloud ice mass to total cloud condensate mass is 90 % (i.e., the phase ratio, PR90) as a useful indicator assessing the model performance to simulate the cloud phase. They found that PR90 in most GCMs is located at lower heights than the satellite observation, implying that most GCMs underestimate cloud

20   liquid mass or overestimate cloud ice mass. Both CAM5 and SAM0 underestimate cloud liquid mass over the Arctic but SAM0 shows some improvements over CAM5 (Fig. 1b).
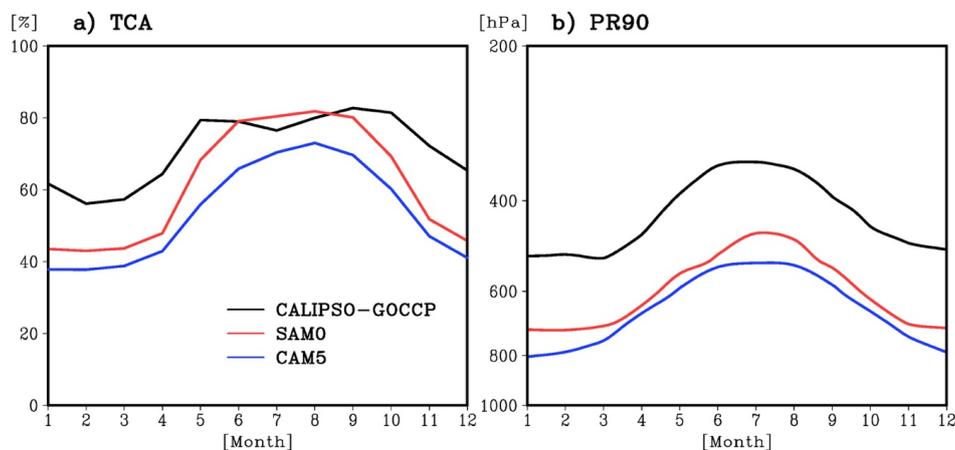
Figure 1. Annual cycles of (a) total cloud fraction (TCA), and (b) the height at which the ratio of ice condensate mass among total condensate mass is 90 % (phase ratio, PR90) averaged over the Arctic area, north of 65° N from CALIPSO-
25   GOCCP observations (black line), SAM0 (red line), and CAM5 (blue line).

Figure 2 shows the annual-mean vertical profiles of grid-mean cloud condensate masses and the difference of cloud fraction between SAM0 and CAM5 averaged over the Arctic area. Compared with CAM5, SAM0 simulates more cloud liquid condensate mass in the lower troposphere but slightly less cloud ice condensate mass throughout the troposphere (Fig. 2b, c). Thus total cloud condensate mass increases (decreases) in the lower troposphere (in the mid-troposphere) from CAM5 to SAM0, respectively, which is responsible for the difference in the cloud fraction (Fig. 2a, d). These changes of cloud characteristics from CAM5 to SAM0 differ from the previously reported impact of the revised ice nucleation scheme (English et al., 2014; Liu et al., 2011; Morrison et al., 2008), which simulated a smaller (larger) low-level (mid-level) cloud fraction. The increase (decrease) of cloud liquid (ice) mass is consistent with the increase of PR90 heights from CAM5 to SAM0 shown in Fig. 1b.
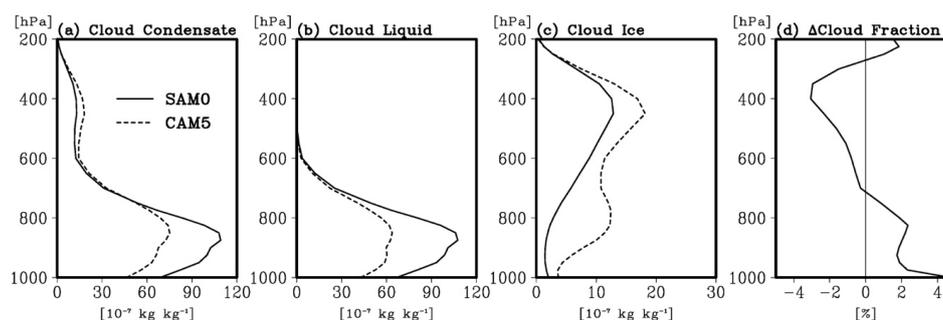
Figure 2. Annual-mean vertical profiles of grid-mean (a) cloud condensate mass (cloud liquid + cloud ice), (b) cloud liquid mass, and (c) cloud ice mass averaged over the Arctic area from SAM0 (solid lines) and CAM5 (dotted lines) and (d) the difference of cloud fraction between SAM0 and CAM5.

In order to understand the physical processes responsible for the increases of cloud fraction and cloud liquid mass in the lower troposphere from CAM5 to SAM0, we plotted the annual-mean vertical profiles of the grid-mean tendencies of cloud liquid and ice condensate masses averaged over the Arctic area from various physical processes (Fig. 3). In both CAM5 and SAM0, two main physical processes generating Arctic cloud liquid condensate are the net condensation of water vapor into cloud liquid (NCD) simulated by the cloud macrophysics scheme and convective detrainment of cloud liquid (DET), while two main depletion processes are the precipitation-sedimentation fallout of cloud condensate (PRS) and WBF conversion of cloud liquid into cloud ice (WBF) simulated by the cloud microphysics scheme (Fig. 3a). In the case of cloud ice condensate, the main sources are the net deposition of water vapor into cloud ice (NCD), WBF, and convective detrainment of cloud ice (DET), while the main sink is PRS (Fig. 3b). Except within the Planetary Boundary Layer (PBL) below 950 hPa, grid-mean tendencies due to subgrid vertical transports of cloud condensates by local symmetric turbulent eddies (PBL) and nonlocal asymmetric turbulent eddies (CON) are generally smaller than other tendencies. Near the surface, the PBL scheme operates as a strong source for cloud liquid owing to downward vertical transport of cloud liquid mass from the cloud layers above (Fig. 3a).
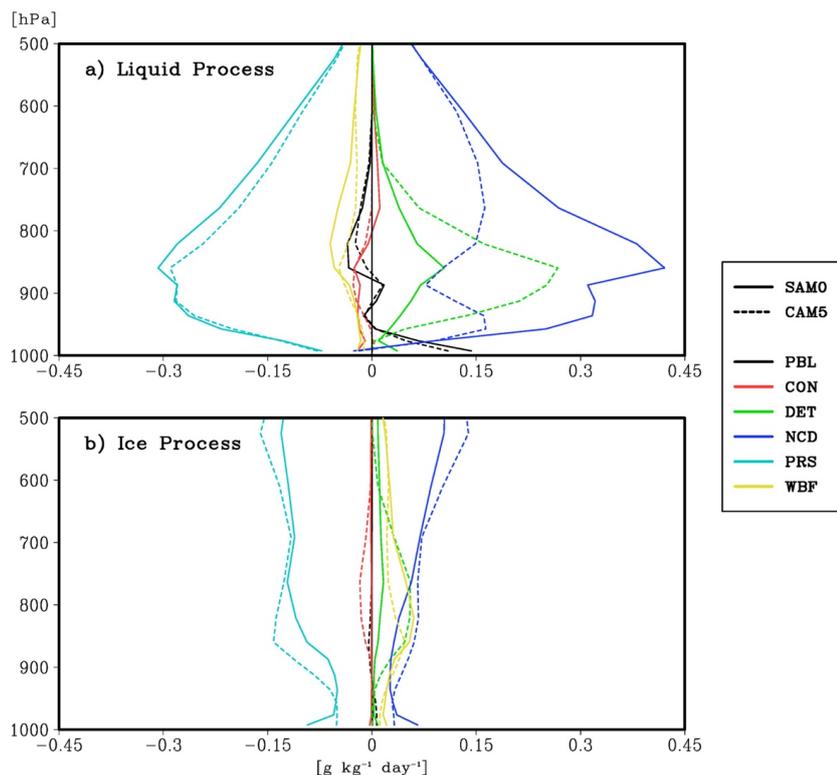
Figure 3. Annual-mean vertical profiles of the grid-mean tendencies of (a) cloud liquid mass and (b) cloud ice mass induced by various moist physics processes from SAM0 (solid lines) and CAM5 (dotted lines). The processes shown are subgrid vertical transport by local symmetric turbulent eddies (PBL, black color); subgrid vertical transport by nonlocal asymmetric turbulent eddies (CON, red); convective detrainment (DET, green); net condensation of water vapor into cloud liquid and net deposition of water vapor into cloud ice (NCD, blue); precipitation-sedimentation fallout (PRS, cyan); and WBF conversion process from cloud liquid mass to cloud ice mass (WBF, yellow).

The largest difference between CAM5 and SAM0 is in NCD and DET, particularly, for cloud liquid. For cloud liquid, SAM0 simulates weaker DET but much stronger NCD than CAM5, such that the sum of NCD and DET simulated by SAM0 is larger than that of CAM5 with the maximum difference of approximately 0.15 g kg^{-1} day^{-1} around the 850 hPa level, where the differences of cloud liquid condensate mass and cloud fraction between CAM5 and SAM0 are also at a maximum (see Fig. 2b). This indicates that the increases of cloud fraction and cloud liquid condensate mass from CAM5 to SAM0 is mainly caused by an enhanced net condensation rate of water vapor into cloud liquid from CAM5 to SAM0. The differences in PBL and CON between CAM5 and SAM0 are relatively small. For cloud ice, the overall production rate simulated by SAM0 is smaller than that of CAM5, mainly due to the decreases in NCD and DET slightly compensated by the increases in WBF and PRS, which leads to the decrease of cloud ice mass as shown in Fig. 2c. The SAM0-simulated WBF tendency is slightly larger than that of CAM5 due in part to the larger cloud liquid mass in SAM0. In summary, the increases of cloud liquid mass, cloud fraction, and PR90 from CAM5 to SAM0 shown in Figs. 1 and 2 (which are improvements) are mainly caused by the enhanced net condensate rate of water vapor into cloud liquid from CAM5 to SAM0. In

accordance with the stronger net condensation rate, the liquid cloud fraction also increases, to satisfy the saturation equilibrium constraint for cloud liquid (see Appendix A of Park et al. (2014)).

The question remains what physical process has caused the increase of net condensate rate from CAM5 to SAM0? According to Park et al. (2014), the horizontal and vertical transports of heat and moisture are the important factors

5   inducing the net condensation of water vapor into cloud liquid both in SAM0 and CAM5. Given that the identical surface boundaries conditions are used in both models (i.e., prescribed sea surface temperature and sea-ice concentration), we speculate that the differences in the large-scale horizontal advection of moisture and temperature from sub-Arctic to Arctic are the reason. Figure 4 shows the differences of zonal-mean meridional transports of heat and moisture in the high latitude region and zonal-mean vertical profiles of water vapor (Q), air

10   temperature (T), and relative humidity (RH) averaged over the Arctic area. The zonal-mean meridional flux is calculated as $\overline{[vX]} = [\overline{v}][\overline{X}] + [\overline{v}^*\overline{X}^*] + [\overline{v'X'}]$, where X = Q or T; v is the meridional velocity; the overbar and prime denote time-mean and departure from the time-mean, respectively; and the square bracket and asterisk denote zonal-mean and departure from the zonal-mean, respectively. The first term on the right-hand side is the flux by the mean meridional circulation, the second term is the flux by stationary eddy, and the last term is the

15   flux by transient eddy. In the midlatitude and subpolar regions, SAM0 simulates poleward fluxes of heat and moisture more than CAM5, particularly, in the lower troposphere (Figs. 4a, e), mainly due to enhanced transports by mean meridional circulation and transient eddies (Figs. 4b-c, f-g). In the northern hemisphere, SAM0 simulates higher pressure in the low latitude region but lower pressure in the high latitude region compared with CAM5, which is an improvement when compared with ERA-Interim observation (Supplementary S1a, b). The circulation

20   change in SAM0 enhances mean meridional circulation and polar jet stream over the higher latitude (Li and Wang, 2003). The associated strengthening of zonal mean meridional wind in the midlatitude region (see the contour lines in Figs. 4b, f) seems to enhance the poleward transports of heat and moisture at near the surface. In addition, enhanced polar jet stream (see the contour lines in Figs. 4c, g) strengthens storm track activity on the periphery of the Arctic circle (between 60° N and 70° N) (Supplementary S1c) and increases the associated poleward

25   transports of heat and moisture by transient eddies.
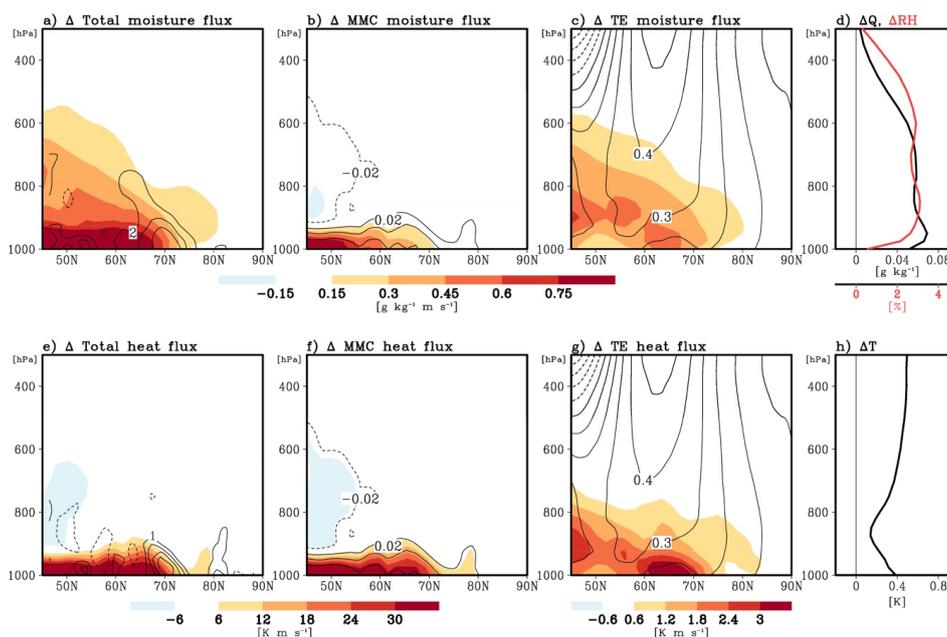
Figure 4. Differences of zonal-mean meridional fluxes of (a, b, and c) moisture and (e, f, and g) heat by (a and e) total processes (i.e., the transported sum by mean meridional circulation, stationary eddies, and transient eddies), (b and f) mean meridional circulation (MMC), and (c and g) transient eddies (TE) between SAM0 and CAM5. Differences of annual zonal-mean vertical profiles (d) water vapor (Q, black) and relative humidity (RH, red), and (h) air temperature (T) averaged over the Arctic area between SAM0 and CAM5. The black lines in (a) and (e) denote the differences of zonal-mean convergence of total moisture flux in 10^{-7} g kg^{-1} s^{-1} and total heat flux in 10^{-5} K s^{-1}, the black lines in (b) and (f) denote the differences of zonal mean meridional wind in m s^{-1}, and the black lines in (c) and (g) denote the differences of zonal-mean zonal wind in m s^{-1} between SAM0 and CAM5, respectively. Most shaded areas exceed a 95 % significance level from the Student t-test.

Consequently, SAM0 simulates higher Q, T, and RH than CAM5 over the Arctic (Figs. 4d, h). Because the liquid cloud fraction is a function of grid-mean RH in both models, this results in the increase of cloud fraction in the lower troposphere, as shown in Fig. 2d. More poleward transport of moisture in SAM0 enhances the net condensation of water vapor into cloud liquid (Park et al., 2014), as shown in Figs. 3a and 2b. In addition, warming associated with enhanced poleward heat transport and condensation heating is likely to reduce the amount of cloud ice mass from CAM5 to SAM0, as shown in Fig. 2c. This, in turn, reduces ice cloud fraction in the mid-troposphere (Fig. 2d) that is formulated as a function of cloud ice condensate mass in both models. The interannual variations of the poleward transport of moisture and net condensation rate of water vapor into Arctic cloud liquid in each model are also highly correlated (Figs. 5a,b), with the correlation coefficients of 0.84 and 0.81 for CAM5 and SAM0, respectively. In addition, in almost all years, SAM0 simulates more poleward moisture flux and higher net condensation rate over the Arctic than CAM5, and the inter-model differences of two variables are also highly correlated (Fig. 5c). In summary, the strengthened mean meridional circulation and transient eddies increase the

poleward transports of heat and moisture, net condensation rate of water vapor into cloud liquid, cloud liquid mass, and cloud fraction from CAM5 to SAM0, sequentially.
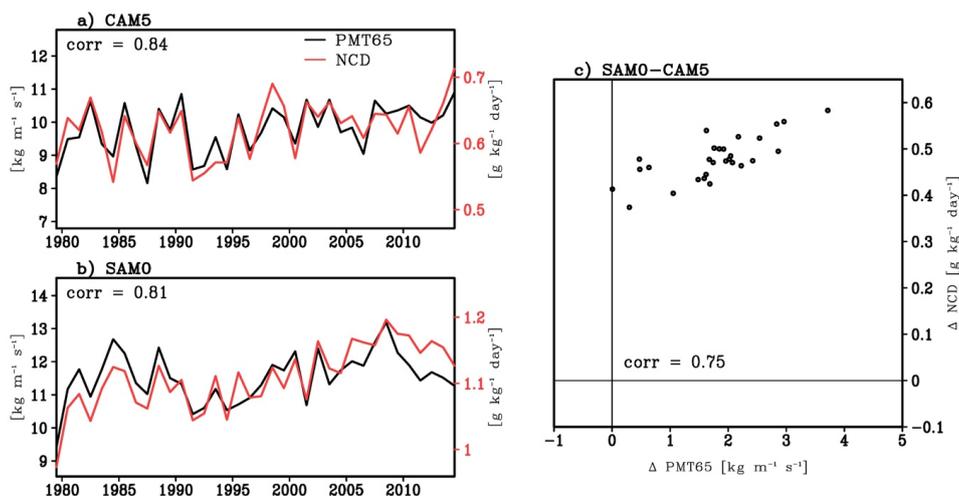
Figure 5. Interannual timeseries of the vertically-integrated annual-mean poleward moisture flux at 65° N (PMT65, black line) and net condensation rate of water vapor into cloud liquid (NCD, red line) averaged over the Arctic area from (a) CAM5 and (b) SAM0, and (c) the scatter plot of the differences of annual-mean PMT65 and NCD between SAM0 and CAM5.

The close association between the Arctic cloudiness and poleward transports of heat and moisture that we showed from the analysis of CAM5 and SAM0 simulations also exist in other climate models. Figure 6 shows the scatter plots between the annual mean meridional transports of heat and moisture at 65° N and Arctic cloudiness and the LWP ratio (i.e., the ratio of cloud liquid water path to total condensate water path, LWP/(LWP+IWP), where IWP denotes ice water path) obtained from the analysis of the various AMIP simulations of CMIP5 models. Wide inter-model spread exists in the TCA, LCA, LWP ratio, and the meridional transports of heat and moisture. However, except for a few outliers (e.g., bcc-csm1-1-m, and MPI-ESM-LR), there is a clear inter-model proportional relationship between the meridional moisture transport and TCA and LCA (Fig. 6a, b). All models simulate consistent poleward moisture transport. However, some models simulate equatorward heat transport at 65° N and the corresponding LWP ratio over the Arctic tends to be smaller than those from the models with poleward heat transport (Fig. 6c). The models with strong poleward moisture transport tend to have strong poleward heat transport as well. The inter-model analysis supports our conclusion that poleward moisture and heat transport is one of the key factors controlling LCA and LWP in the Arctic.
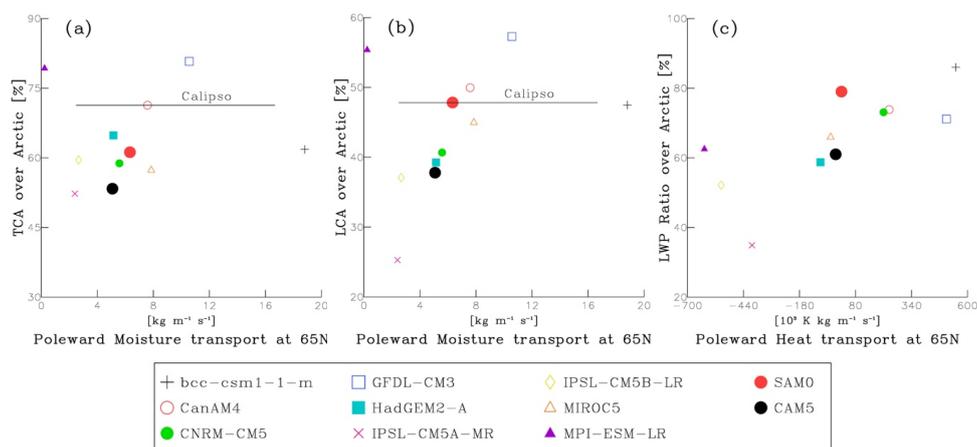
Figure 6. Scatter plots among the annual mean poleward fluxes of moisture and heat integrated over the vertical layers (1000–700hPa) at 65° N, cloud fractions, and the LWP ratio averaged over the Arctic area, obtained from various AMIP simulations of CMIP5 models, CAM5 and SAM0. The black lines in (a) and (b) denote the observed TCA and LCA, respectively, obtained from CALIPSO-GOCCP data.

3.2 Impact of Arctic clouds on the Arctic climate

Figure 7 shows biases of TCA, upward LW radiation flux at the top of the atmosphere (TOA) (FLUT), and T_{2m} during wintertime obtained from CAM5 and SAM0. As shown in the figure, CAM5 suffers from the negative biases of TCA, FLUT, and T_{2m} during December-January-February (DJF) (Fig. 7, left panel). In the Arctic during winter, a strong temperature inversion exists over the land and the sea-ice region in the lower troposphere, such that less LCA in CAM5 reduces FLUT and also downward LW radiation at the surface (FLDS), resulting in colder near-surface air than the observation. Compared with CAM5, SAM0 simulates more TCA, FLUT, and T_{2m} over the whole Arctic (Fig. 7, center panel), such that the negative biases of TCA, FLUT, and T_{2m} in CAM5 are alleviated in SAM0 (Fig. 7, right panel). Over the ocean where temperature inversion does not exist, more LCA in SAM0 results in more FLUT than CAM5 (Fig. 7e). It is not shown here, but SAM0 also simulates stronger FLDS than CAM5 over the entire Arctic, as expected.
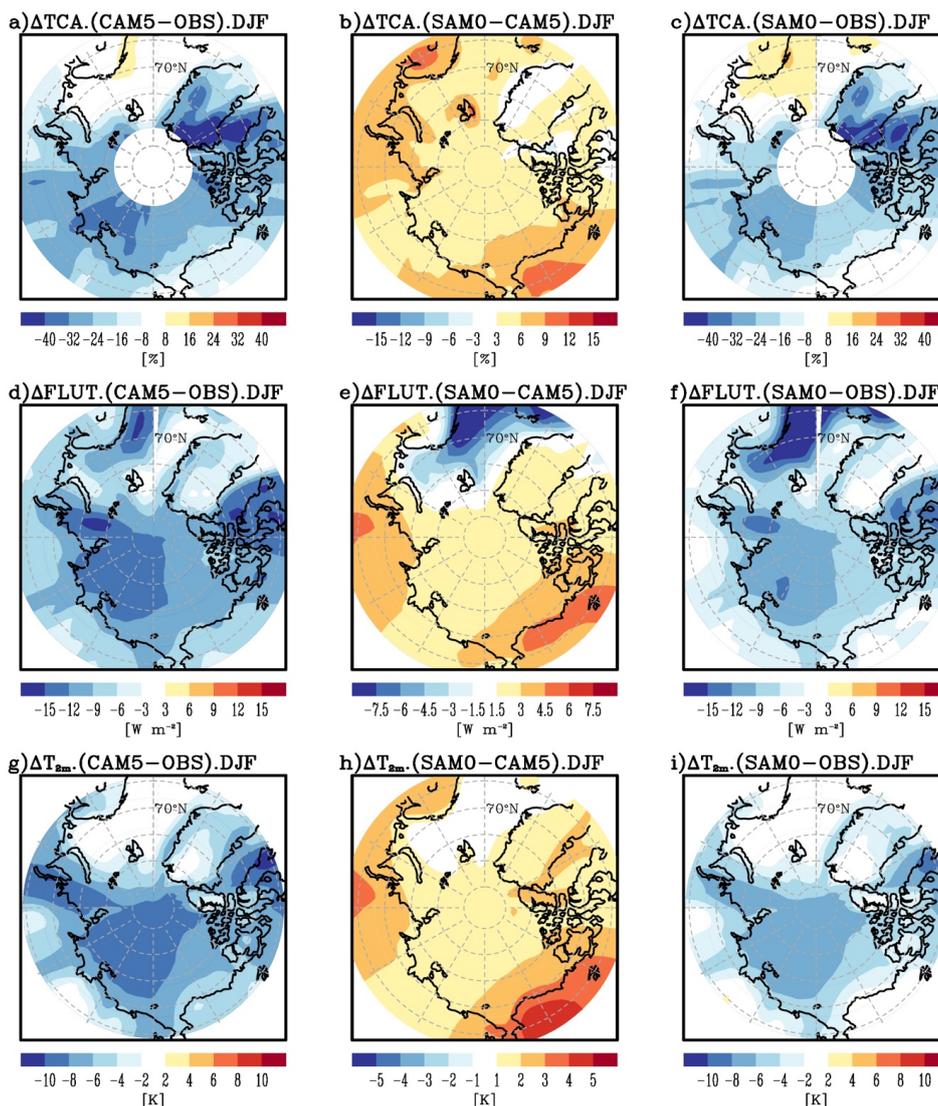
Figure 7. Biases of (upper) TCA against the CALIPSO–GOCCP observation, (middle) upward longwave (LW) radiative flux at TOA (FLUT) against the CERES–EBAF observation, and (lower) near-surface air temperature at a 2 m height (T_{2m}) against the ERA-interim reanalysis during DJF obtained from (left) CAM5 and (right) SAM0; and (center) differences of each variable between SAM0 and CAM5. Most shaded areas in (b), (e), and (h) exceed a 95 % significance level from the Student t-test.

Not only the biases during DJF, a summertime biases of TCA, shortwave cloud radiative forcing at TOA (SWCF), and T_{2m} are also reduced from CAM5 to SAM0 (Fig. 8). In most Arctic areas except for some portions of the northern continents, CAM5 has the negative biases of TCA (mainly LCA) during June-July-August (JJA) (Fig. 8a). SAM0 simulates more TCA than CAM5 (Fig. 8b), such that most of the negative TCA biases in CAM5 over the Arctic sea ice and open ocean areas disappear (Fig. 8c). With more LCA than CAM5, SAM0 simulates more net LW radiation at the surface (FLNS, Fig. 9b). Due to the high albedo of underlying sea ice and snow in the

vicinity of the Arctic pole, net SW radiation at the surface (FSNS) does not change much there; however, FSNS decreases substantially in the surrounding regions of the Arctic pole (Fig. 9a). Overall, the increase of FLNS dominates over the decrease of FSNS in the Arctic pole, while the opposite is true in the surrounding regions (Fig. 9b, c). The associated increase of T_{2m} from CAM5 to SAM0 in the Arctic pole (Fig. 8h) decreases snow depth

5   and surface albedo, while the opposite increases of snow depth and surface albedo occur in the surrounding continental area (Fig. 9d, e). The enhanced SWCF cooling near the Arctic pole in SAM0 shown in Fig. 8e is the combined results of the increased LCA and decreased snow depth and surface albedo. If the Arctic sea ice fraction is allowed to change in response to the charges of overlying atmospheric conditions (e.g., coupled simulation), SAM0 is likely to simulate less sea ice fraction than CAM5 due to more LCA and warmer near-surface air

10   temperature, which can be further accelerated by the positive surface albedo feedback (Holland and Bitz, 2003). In fact, Park et al. (2019) found that SAM0 simulates less sea ice fraction than the Community Earth System Model version 1 (CESM1, a coupled model of CAM5, Hurrell et al., 2013) over the Arctic in the 20th century coupled simulation.
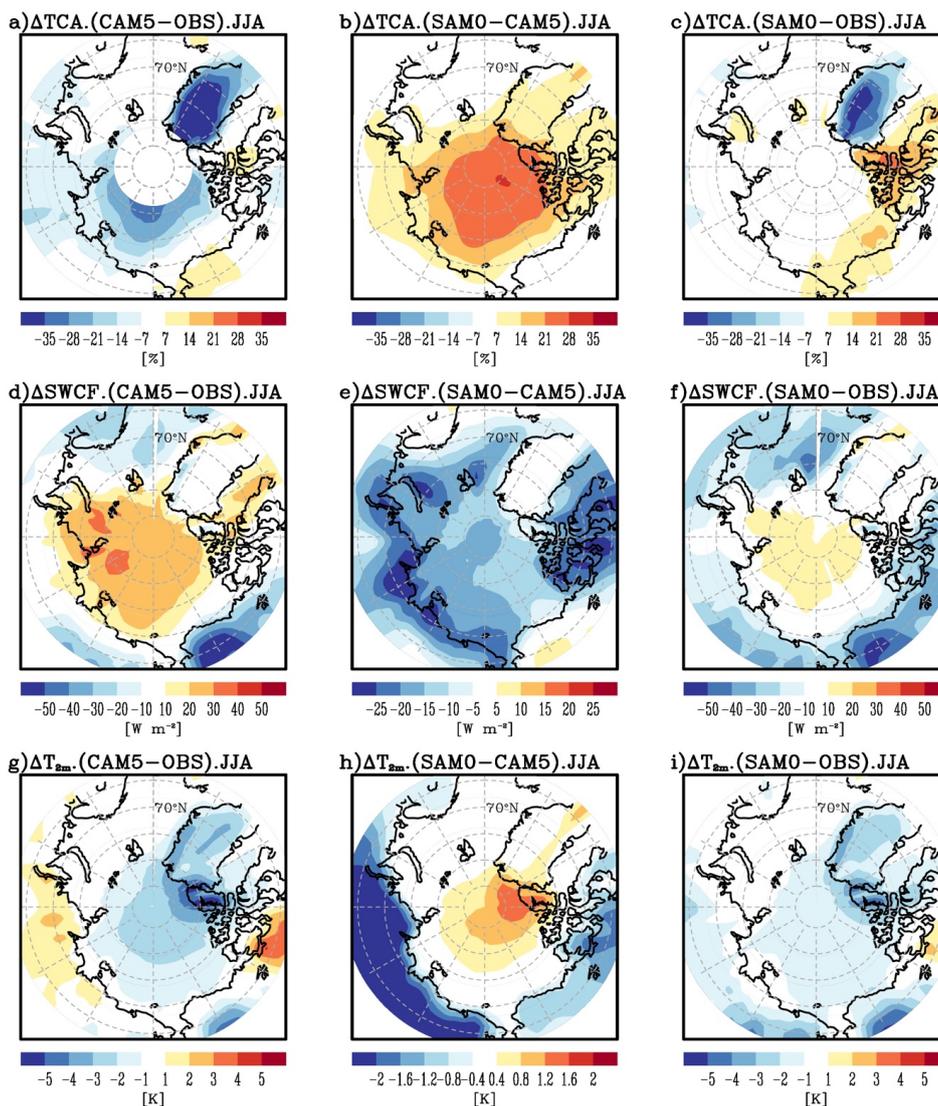
Figure 8. Identical with Fig. 7, except for shortwave cloud radiative forcing at TOA (SWCF) in the middle panel and during JJA. Most shaded areas in (b), (e), and (h) exceed a 95 % significance level from the Student t-test.
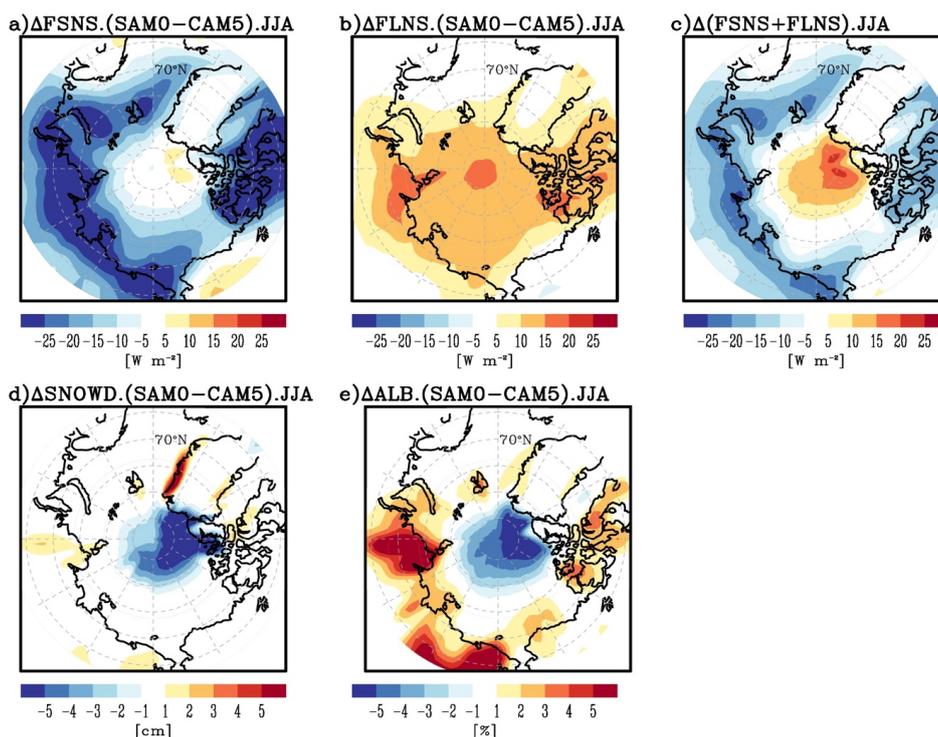
Figure 9. Differences of (a) net SW flux at the surface (FSNS), (b) net LW flux at the surface (FLNS), (c) sum of FSNS and FLNS, (d) snow depth (SNOWD), and (e) surface albedo (ALB) during JJA between SAM0 and CAM5. Most shaded areas exceed a 95 % significance level from the Student t-test.

4. Summary and Discussion

Many GCMs suffer from the cold bias over the Arctic, which has been speculated to be caused by the biases of radiation in association with the underestimated cloud fraction and cloud liquid mass over the Arctic. As an attempt to address this issue, we compared various aspects of the Arctic clouds and climate in two different AMIP simulations generated by CAM5 and SAM0.

Similar to other GCMs and previous studies, CAM5 underestimates cloud fraction and cloud liquid mass in the Arctic lower troposphere throughout the year. SAM0 remedies these problems, although the biases are still persisting. Our analysis showed that this improvement in the Arctic cloud simulation with SAM0 is mainly due to stronger net condensation rate of water vapor into cloud liquid, which in turn, was due to enhanced poleward transports of heat and moisture by mean meridional circulation and transient eddies. A new unified convection scheme (UNICON) in SAM0 seems to strengthen and shift poleward the zonal mean meridional circulation, polar jet stream, and associated synoptic storm activity on the periphery of the Arctic circle. The proportional relationship between the Arctic cloudiness and meridional transports of heat and moisture in CAM5 and SAM0 also exists in a set of CMIP5 models. In association with the deficient simulations of cloud fraction and cloud liquid mass, CAM5 suffers from the negative bias of near-surface air temperature throughout the year. With more cloud fraction and cloud liquid mass, SAM0 also remedies the cold temperature biases in the Arctic mainly by

enhancing downward LW radiation at the surface, in consistency with the hypothesis suggested by previous studies (Barton et al., 2014; Chan and Comiso, 2013; Klocke et al., 2011; Pithan and Mauritsen, 2014; Walsh and Chapman, 1998). Our study indicates that the proper simulation of poleward transports of heat and moisture from sub-Arctic to Arctic is one of the key factors necessary to improve the simulations of Arctic clouds and climate.

5 The authors are continuously working on to further reduce the remaining biases of Arctic clouds and climate by controlling convective activity simulated by UNICON and incorporating an improved ice nucleation scheme suggested by previous studies.

Author Contributions

E.-H. Baek performed the overall numerical experiments and analysis. S. Park developed and provided SAM0

10 and CAM5, and helped to analyze the simulation results. B.-M. Kim designed the project and helped to analyze the CMIP5 models. All authors contributed to conducting analyses.

Competing interests

The authors declare that they have no conflict of interest.

Acknowledgments

15 This work was supported by the Korea Polar Research Institute project, titled 'Development and Application of the Korea Polar Prediction System (KPOPS) for Climate Change and Disastrous Weather Events (PE19130)'. S. Park is supported by the Creative-Pioneering Researchers Program through the Seoul National University (SNU) (grant number 3345-20180015). B.-M. Kim is supported by the Korea Meteorological Administration Research and Development Program (grant number KMI2018-03810). J.-H. Jeong is supported by the Korea

20 Meteorological Administration Research and Development Program (grant number KMI2018-01013).

References

Barton, N. P., Klein, S. A. and Boyle, J. S.: On the Contribution of Longwave Radiation to Global Climate Model Biases in Arctic Lower Tropospheric Stability, J. Clim., 27, 7250–7269, doi:10.1175/JCLI-D-14-00126.1, 2014.

25 Bergeron, T.: Proces Verbaux de l'Association de Meteorologie (ed. Duport, P.), International Union of Geodesy and Geophysics., 1935.

Boe, J., Hall, A. and Qu, X.: Current GCMs' Unrealistic Negative Feedback in the Arctic, J. Clim., 22(17), 4682–4695, doi:10.1175/2009JCLI2885.1, 2009.

de Boer, G., Chapman, W. L., Kay, J. E., Medeiros, B., Shupe, M. D., Vavrus, S. and Walsh, J. E.: A

30 Characterization of the Present-Day Arctic Atmosphere in CCSM4, J. Clim., 25, 2676–2695, doi:10.1175/JCLI-D-11-00228.1, 2012.

Cesana, G. and Chepfer, H.: How well do climate models simulate cloud vertical structure? A comparison between CALIPSO-GOCCP satellite observations and CMIP5 models, Geophys. Res. Lett., 39(20), 1–6, doi:10.1029/2012GL053153, 2012.

Cesana, G., Waliser, D. E., Jiang, X. and Li, J.-L. F.: Multi-model evaluation of cloud phase transition using

5   satellite and reanalysis data, J. Geophys. Res. Atmos., (JUNE), n/a-n/a, doi:10.1002/2014JD022932, 2015.

Chan, M. A. and Comiso, J. C.: Arctic cloud characteristics as derived from MODIS, CALIPSO, and cloudsat, J. Clim., 26(10), 3285–3306, doi:10.1175/JCLI-D-12-00204.1, 2013.

Chapman, W. L. and Walsh, J. E.: Simulations of Arctic temperature and pressure by global coupled models, J. Clim., 20(4), 609–632, doi:10.1175/JCLI4026.1, 2007.

10   Chepfer, H., Bony, S., Winker, D., Cesana, G., Dufresne, J. L., Minnis, P., Stubenrauch, C. J. and Zeng, S.: The GCM-oriented CALIPSO cloud product (CALIPSO-GOCCP), J. Geophys. Res. Atmos., 115(5), 1–13, doi:10.1029/2009JD012251, 2010.

Dee, D. P., Uppala, S. M., Simmons, A. J., Berrisford, P., Poli, P., Kobayashi, S., Andrae, U., Balmaseda, M. A., Balsamo, G., Bauer, P., Bechtold, P., Beljaars, A. C. M., van de Berg, L., Bidlot, J., Bormann, N., Delsol,

15   C., Dragani, R., Fuentes, M., Geer, A. J., Haimberger, L., Healy, S. B., Hersbach, H., H??lm, E. V., Isaksen, L., K??llberg, P., K??hler, M., Matricardi, M., Mcnally, A. P., Monge-Sanz, B. M., Morcrette, J. J., Park, B. K., Peubey, C., de Rosnay, P., Tavolato, C., Th??paut, J. N. and Vitart, F.: The ERA-Interim reanalysis: Configuration and performance of the data assimilation system, Q. J. R. Meteorol. Soc., 137(656), 553–597, doi:10.1002/qj.828, 2011.

20   Deser, C., Walsh, J. E. and Timlin, M. S.: Arctic Sea Ice Variability in the Context of Recent Atmospheric Circulation Trends, J. Clim., 13, 617–633, 2000.

English, J. M., Kay, J. E., Gettelman, A., Liu, X., Wang, Y., Zhang, Y. and Chepfer, H.: Contributions of clouds, surface albedos, and mixed-phase ice nucleation schemes to Arctic radiation biases in CAM5, J. Clim., 27(13), 5174–5197, doi:10.1175/JCLI-D-13-00608.1, 2014.

25   English, J. M., Gettelman, A. and Henderson, G. R.: Arctic radiative fluxes: Present-day biases and future projections in CMIP5 models, J. Clim., 28(15), 6019–6038, doi:10.1175/JCLI-D-14-00801.1, 2015.

Eyring, V., Bony, S., Meehl, G. A., Senior, C. A., Stevens, B., Stouffer, R. J. and Taylor, K. E.: Overview of the Coupled Model Intercomparison Project Phase 6 (CMIP6) experimental design and organization, Geosci. Model Dev., 9(5), 1937–1958, doi:10.5194/gmd-9-1937-2016, 2016.

30   Findeisen, W.: Kolloid-Meteorologische, 2nd ed., Am. Meteorol. Soc., Boston, Mass., 1938.

Holland, M. M. and Bitz, C. M.: Polar amplification of climate change in coupled models, Clim. Dyn., 21(3–4), 221–232, doi:10.1007/s00382-003-0332-6, 2003.

Hurrell, J. W., Holland, M. M., Gent, P. R., Ghan, S., Kay, J. E., Kushner, P. J., Lamarque, J. F., Large, W. G., Lawrence, D., Lindsay, K., Lipscomb, W. H., Long, M. C., Mahowald, N., Marsh, D. R., Neale, R. B., Rasch,

35   P., Vavrus, S., Vertenstein, M., Bader, D., Collins, W. D., Hack, J. J., Kiehl, J. and Marshall, S.: The community earth system model: A framework for collaborative research, Bull. Am. Meteorol. Soc., 94(9), 1339–1360, doi:10.1175/BAMS-D-12-00121.1, 2013.

Jiang, H., Cotton, W. R., Pinto, J. O., Curry, J. A. and Weissbluth, M. J.: Cloud Resolving Simulations of Mixed-Phase Arctic Stratus Observed during BASE: Sensitivity to Concentration of Ice Crystals and Large-

Scale Heat and Moisture Advection, J. Atmos. Sci., 57(13), 2105–2117, doi:10.1175/1520-0469(2000)057<2105:CRSOMP>2.0.CO;2, 2000.

Johannessen, O. M., Kuzmina, S. I., Bobylev, L. P., Martin, W., Johannessen, O. M., Kuzmina, S. I. and Bobylev, L. P.: Tellus A : Dynamic Meteorology and Oceanography Surface air temperature variability and trends in the Arctic : new amplification assessment and regionalisation Surface air temperature variability and trends in the Arctic : new amplification assessment and regionalisation, 0870(May), doi:10.3402/tellusa.v68.28234, 2016.

Karlsson, J. and Svensson, G.: Consequences of poor representation of Arctic sea-ice albedo and cloud-radiation interactions in the CMIP5 model ensemble, Geophys. Res. Lett., 40(16), 4374–4379, doi:10.1002/grl.50768, 2013.

Kay, J. E., Hillman, B. R., Klein, S. A., Zhang, Y., Medeiros, B., Pincus, R., Gettelman, A., Eaton, B., Boyle, J., Marchand, R. and Ackerman, T. P.: Exposing global cloud biases in the Community Atmosphere Model (CAM) using satellite observations and their corresponding instrument simulators, J. Clim., 25(15), 5190–5207, doi:10.1175/JCLI-D-11-00469.1, 2012.

Kay, J. E., Bourdages, L., Miller, N. B., Morrison, A., Yettella, V., Chepfer, H. and Eaton, B.: Evaluating and improving cloud phase in the Community Atmosphere Model version 5 using spaceborne lidar observations, J. Geophys. Res. Atmos., 121(8), 4162–4176, doi:10.1002/2015JD024699, 2016.

King, M. D., Platnick, S., Yang, P., Arnold, G. T., Gray, M. A., Riedi, J. C., Ackerman, S. A. and Liou, K.-N.: Remote Sensing of Liquid Water and Ice Cloud Optical Thickness and Effective Radius in the Arctic : Application of Airborne Multispectral MAS Data, J. Atmos. Ocean. Technol., 21, 857–875, 2004.

Klocke, D., Pincus, R. and Quaas, J.: On constraining estimates of climate sensitivity with present-day observations through model weighting, J. Clim., 24(23), 6092–6099, doi:10.1175/2011JCLI4193.1, 2011.

Korolev, A. and Field, P. R.: The Effect of Dynamics on Mixed-Phase Clouds: Theoretical Considerations, J. Atmos. Sci., 65(1), 66–86, doi:10.1175/2007JAS2355.1, 2008.

Kug, J.-S., Jeong, J.-H., Jang, Y.-S., Kim, B.-M., Folland, C. K., Min, S.-K. and Son, S.-W.: Two distinct influences of Arctic warming on cold winters over North America and East Asia, Nat. Geosci., 8(10), 759–762, doi:10.1038/ngeo2517, 2015.

Li, J. and Wang, J. X. L.: A modified zonal index and its physical sense, Geophys. Res. Lett., 30(12), 1–4, doi:10.1029/2003GL017441, 2003.

Liu, X., Xie, S., Boyle, J., Klein, S. A., Shi, X., Wang, Z., Lin, W., Ghan, S. J., Earle, M., Liu, P. S. K. and Zelenyuk, A.: Testing cloud microphysics parameterizations in NCAR CAM5 with ISDAC and M-PACE observations, J. Geophys. Res. Atmos., 116(24), 1–18, doi:10.1029/2011JD015889, 2011.

Loeb, N. G., Wielicki, B. A., Doelling, D. R., Smith, G. L., Keyes, D. F., Kato, S., Manalo-Smith, N. and Wong, T.: Toward optimal closure of the Earth's top-of-atmosphere radiation budget, J. Clim., 22(3), 748–766, doi:10.1175/2008JCLI2637.1, 2009.

Lu, J. and Cai, M.: Seasonality of polar surface warming amplification in climate simulations, Geophys. Res. Lett., 36(August), 1–6, doi:10.1029/2009GL040133, 2009.

Madden, R. A. and Julian, P. R.: Detection of a 40–50 Day Oscillation in the Zonal Wind in the Tropical Pacific, J. Atmos. Sci., 28(5), 702–708, doi:10.1175/1520-0469(1971)028<0702:DOADOI>2.0.CO;2, 1971.

Morrison, H., Pinto, J. O., Curry, J. A. and McFarquhar, G. M.: Sensitivity of modeled arctic mixed-phase stratocumulus to cloud condensation and ice nuclei over regionally varying surface conditions, J. Geophys. Res. Atmos., 113(5), 1–16, doi:10.1029/2007JD008729, 2008.

Morrison, H., de Boer, G., Feingold, G., Harrington, J., Shupe, M. D. and Sulia, K.: Resilience of persistent Arctic mixed-phase clouds, Nat. Geosci., 5(1), 11–17, doi:10.1038/ngeo1332, 2011.

Neale, R. B., Gettelman, A., Park, S., Chen, C., Lauritzen, P. H., Williamson, D. L., Conley, A. J., Kinnison, D., Marsh, D., Smith, A. K., Vitt, F., Garcia, R., Lamarque, J., Mills, M., Tilmes, S., Morrison, H., Cameron-smith, P., Collins, W. D., Iacono, M. J., Easter, R. C., Liu, X., Ghan, S. J., Rasch, P. J. and Taylor, M. a: Description of the NCAR Community Atmosphere Model (CAM 5.0). NCAR Technical Notes., Tech. Note NCAR/TN-464+STR, 214, doi:10.5065/D6N877R0., 2012.

Park, S.: A Unified Convection Scheme, UNICON. Part I. Formulation, J. Atmos. Sci., (Lcl), 140808112307001, doi:10.1175/JAS-D-13-0234.1, 2014a.

Park, S.: A Unified Convection Scheme, UNICON. Part II. Simulation, J. Atmos. Sci., (Lcl), 140808112307001, doi:10.1175/JAS-D-13-0234.1, 2014b.

Park, S. and Bretherton, C. S.: The University of Washington shallow convection and moist turbulence schemes and their impact on climate simulations with the community atmosphere model, J. Clim., 22(12), 3449–3469, doi:10.1175/2008JCLI2557.1, 2009.

Park, S., Bretherton, C. S. and Rasch, P. J.: Integrating Cloud Processes in the Community Atmosphere Model, Version 5, J. Clim., 27(18), 6821–6856, doi:10.1175/JCLI-D-14-00087.1, 2014.

Park, S., Baek, E.-H., Kim, B.-M. and Kim, S.-J.: Impact of detrained cumulus on climate simulated by the Community Atmosphere Model Version 5 with a unified convection scheme, J. Adv. Model. Earth Syst., 6, 513–526, doi:10.1002/2016MS000877, 2017.

Park, S., Shin, J., Kim, S., Oh, E., and Kim, Y.: Global climate simulated by the Seoul National University Atmosphere Model Version 0 with a Unified Convection Scheme (SAM0-UNICON), J. Clim., Accepted. 2019.

Pithan, F. and Mauritsen, T.: Arctic amplification dominated by temperature feedbacks in contemporary climate models, Nat. Geosci., 7(February), 2–5, doi:10.1038/NGEO2071, 2014.

Pithan, F., Medeiros, B. and Mauritsen, T.: Mixed-phase clouds cause climate model biases in Arctic wintertime temperature inversions, Clim. Dyn., 43(1–2), 289–303, doi:10.1007/s00382-013-1964-9, 2014.

Prenni, A. J., DeMott, P. J., Kreidenweis, S. M., Harrington, J. Y., Avramov, A., Verlinde, J., Tjernström, M., Long, C. N. and Olsson, P. Q.: Can Ice-Nucleating Aerosols Affect Arctic Seasonal Climate?, Bull. Am. Meteorol. Soc., 88(4), 541–550, doi:10.1175/BAMS-88-4-541, 2007.

Screen, J. A. and Simmonds, I.: The central role of diminishing sea ice in recent Arctic temperature amplification., Nature, 464(7293), 1334–1337, doi:10.1038/nature09051, 2010.

Screen, J. A. and Simmonds, I.: Exploring links between Arctic amplification and mid-latitude weather, Geophys. Res. Lett., 40(5), 959–964, doi:10.1002/grl.50174, 2013.

Sedlar, J. and Tjernström, M.: Stratiform Cloud—Inversion Characterization During the Arctic Melt Season, Boundary-Layer Meteorol., 132(3), 455–474, doi:10.1007/s10546-009-9407-1, 2009.

Serreze, M. C. and Barry, R. G.: Processes and impacts of Arctic amplification : A research synthesis, Glob. Planet. Change, 77(1–2), 85–96, doi:10.1016/j.gloplacha.2011.03.004, 2011.

Shupe, M. D. and Intrieri, J. M.: Cloud radiative forcing of the Arctic surface: The influence of cloud properties, surface albedo, and solar zenith angle, J. Clim., 17(3), 616–628, doi:10.1175/1520-0442(2004)017<0616:CRFOTA>2.0.CO;2, 2004.

Shupe, M. D., Kollias, P., Persson, P. O. G. and McFarquhar, G. M.: Vertical Motions in Arctic Mixed-Phase Stratiform Clouds, J. Atmos. Sci., 65(4), 1304–1322, doi:10.1175/2007JAS2479.1, 2008.

Shupe, M. D., Walden, V. P., Eloranta, E., Uttal, T., Campbell, J. R., Starkweather, S. M. and Shiobara, M.: Clouds at Arctic atmospheric observatories. Part I: Occurrence and macrophysical properties, J. Appl. Meteorol. Climatol., 50(3), 626–644, doi:10.1175/2010JAMC2467.1, 2011.

Solomon, A., Shupe, M. D., Persson, P. O. G. and Morrison, H.: Moisture and dynamical interactions maintaining decoupled Arctic mixed-phase stratocumulus in the presence of a humidity inversion, Atmos. Chem. Phys., 11(19), 10127–10148, doi:10.5194/acp-11-10127-2011, 2011.

Taylor, K. E., Stouffer, R. J. and Meehl, G. A.: An overview of CMIP5 and the experiment design, Bull. Am. Meteorol. Soc., 93(4), 485–498, doi:10.1175/BAMS-D-11-00094.1, 2012.

Walsh, J. E. and Chapman, W. L.: Arctic cloud-radiation-temperature associations in observational data and atmospheric reanalyses, J. Clim., 11(11), 3030–3045, doi:10.1175/1520-0442(1998)011<3030:ACRTAI>2.0.CO;2, 1998.

Wegener, A.: Thermodynamik der Atmosphare, Barth., edited by J. A. Barth, Leipzig, Germany., 1911.

Wielicki, B. A., Barkstrom, B. R., Harrison, E. F., Lee, R. B., Smith, G. L. and Cooper, J. E.: Clouds and the Earth's Radiant Energy System (CERES): An Earth Observing System Experiment, Bull. Am. Meteorol. Soc., 77(5), 853–868, doi:10.1175/1520-0477(1996)077<0853:CATERE>2.0.CO;2, 1996.

Wu, Y. and Smith, K. L.: Response of Northern Hemisphere Midlatitude Circulation to Arctic Amplification in a Simple Atmospheric General Circulation Model, J. Clim., 29(6), 2041–2058, doi:10.1175/JCLI-D-15-0602.1, 2016.

Xie, S., Liu, X., Zhao, C. and Zhang, Y.: Sensitivity of CAM5-Simulated Arctic Clouds and Radiation to Ice Nucleation Parameterization, J. Clim., 26, 5981–5999, doi:10.1175/JCLI-D-12-00517.1, 2013.

Zhang, G. J. and McFarlane, N. A.: Role of convective scale momentum transport in climate simulation, J. Geophys. Res. Atmos., 100(D1), 1417–1426, doi:10.1029/94JD02519, 1995.